PEER REVIEW, Vol. 6, Nº 6, 2024
DOI: 10.53660/PRW-1957-3610
ISSN: 1541-1389

Production of nanocomposite based on PETG, manufactured by 3D printing, to combat the Sars-Cov-2 virus

Produção de nanocompósito à base de PETG, fabricados por meio de impressão 3D, para combater o vírus Sarg-Cov-2

Thais da Silva Santos
ORCID: https://orcid.org/0000-0001-7373-0029
Universidade do Estado do Amazonas, Brasil
E-mail: thais.santos19991424@gmail.com
Joziane Silva da Cunha
ORCID: https://orcid.org/0009-0006-8530-7686
Universidade do Estado do Amazonas, Brasil
E-mail: jozianecunha.uea@gmail.com
José Costa de Macêdo Neto
ORCID: https://orcid.org/0000-0003-1155-0027
Universidade do Estado do Amazonas, Basil
E-mail: jmacedo@uea.edu.br
Waldeir Silva Dias
ORCID: https://orcid.org/0009-0008-8932-0209
Universidade Federal do Amazonas, Basil
E-mail: waldeirs.dias@gmail.com

ABSTRACT

With the collapse of the COVID-19 pandemic, it was necessary to explore new materials with resistance to SARS-CoV-2 of lower cost and effective and easy production methods, such as 3D printing. The objective was to produceand characterize filaments for 3D printing using PETG and copper nanoparticles (NCu) aiming at obtaining a virucidal surface. Nanocomposites were made with the addition of 0.75% and 1% of NCu and pure PETG. After printing, mechanical tests of nanoindentation, thermogravimetric analyses (TGA), digital optical microscopies andFourier transform infrared spectroscopies (FTIR) were performed. The results showed a 48% increase in the elastic modulus for the 0.75% and 1% nanocomposites compared to pure PETG. In the TGA, the results were significantfor the nanocomposites with the addition of 1% of NCu compared to pure PETG. In the chemical composition byFTIR spectrum, there were no significant changes.

Keywords: PETG; 3D printing; Copper nano particle.

Recebido: 02/01/2024 | Aceito: 05/03/2024 | Publicado: 09/03/2024

RESUMO

Com o colapso da pandemia do COVID-19, foi necessário explorar novos materiais com resistência ao SARS- CoV-2 de menor custo e métodos de produção eficazes e fáceis, como a impressão 3D. O objetivo foi produzir e caracterizar filamentos para impressão 3D utilizando PETG e nanopartículas de cobre (NCu) visando à obtenção de superfície virucida. Foram feitos nanocompósitos com adição de 0,75% e 1% de NCu e PETG puro. Após a impressão, foram realizados testes mecânicos de nanoindentação, análises termogravimétricas (TGA), microscopias ópticas digitais e espectroscopias de infravermelho por transformada de Fourier (FTIR). Os resultados mostraram um aumento de 48% no módulo de elasticidade para os nanocompósitos de 0,75% e 1% emrelação ao PETG puro. Na TGA, os resultados mostraram-se significativos para os nanocompósitos com adição de 1% de NCu em comparação com o PETG puro. Na composição química por espectro de FTIR, não houve mudanças significativas.

Palavras-chave: PETG; Impressão 3D; Nano partícula de Cobre.

INTRODUCION

The SARS-CoV-2 is a virus of zoonotic origin, first detected in Wuhan, Hubei province, China in early December 2019, according to the Pan American Health Organization (OPAS, 2019). In their work, (Jaimes et al., 2020, pp. 1-6) reported that the rapid spread of this virus is due to a protein called furin, present on the surface of the virus and also present in various human tissues, which can explain the rapid infection of cells. The same protein is chosen by Ebola and HIV, for example. Therefore, the National Health Surveillance Agency (ANVISA, 2020) recommends cleaning and disinfecting potentially contaminated environments with germicidal disinfectants.

To combat infections caused by microorganisms, the use of antimicrobial agents has been an option for the development of environments that promote health and well-being. To prevent the degradative processes generated by microorganisms, the use of plastics with antimicrobial properties is an excellent option, being the subject of several studies from academic and industrial perspectives (De Paoli, M. A., 2017). This refers to nanocomposites with a polymeric matrix of inorganic/organic nanometric interfaces (March 11, 2020).

The ability of copper to donate and accept electrons in a continuous process is a crucial element for antibacterial activity and studies report that the mechanism of copper toxicity is linked to the release of hydroperoxide radicals. Copper easily catalyzes reactions that result in the production of hydroxyl radicals through Fenton Reactions (Reaction 1) and Haber-Weiss (Reactions 2 and 3) (Palza, H et al, 2015). The polymeric material that has been gaining ground among users of the 3D printing community is PETG, especially when there is a need to build flexible and durable parts. It is characterized by being a modified version of PET, in which the “G” means “glycol modified”, being added to the composition of the material during polymerization (ANATOL LOCKER ALL 3DP, 2017).

This work aims to use copper nanoparticles in a PETG polymer matrix for the production of filaments for 3D printing that can be used in the production of PPE parts and objects with high physical contact. The mechanical properties obtained in this work were made from the tensile test in (Young's modulus), thermogravimetric analyses (TGA), nano hardness test and fractographic analysis by scanning electron microscopy (SEM) and chemical composition (FTIR) were obtained in this work.

MATERIALS AND METHODS

Materials

The materials obtained were provided by the company Amcor da Amazônia with PETG (in filaments) of natural color and the copper nanoparticle that had a diameter close to 100 nmand purity above 99%, was provided by the Company Hongwu International Group, China, shown in Figure 1 (a) and (b) and the pure PETG filament was previously crushed in a minigranulator (Model AX, Plastics, Brazil). Figure 1 (c).

Figure 1 - Natural PETG polymers, (a) Copper alloy nanoparticles, respectively, (b) Mini granulator (AXPlastics) (c).

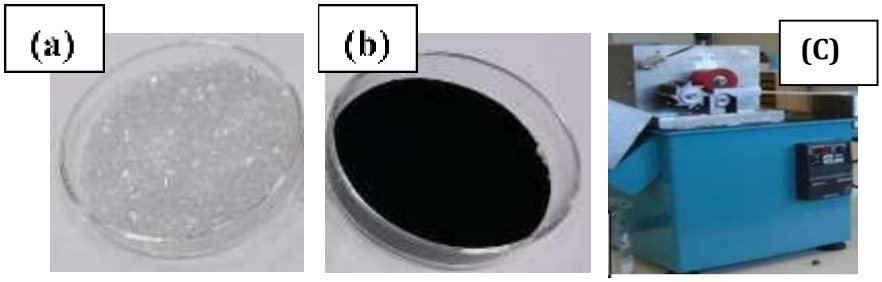

Source: Santos et al (2021).

Production of filaments and specimens in 3D printing

The shredded PETG polymer was dried in an oven for 2 h at 50 ºC before being mixed with the nanoparticles. The concentrations of copper nanoparticles (NCu) were 0.75 and 1.00%by weight. There was a pre-mixing of the materials, and they were processed in an extruder (MR.16:26, AX, Plastics, Brazil) at 180°C and rotation of 50 rpm to obtain the filaments. Then,the SolidWorck 3D academic software was used to design the desired parts with measurements according to ASTM D638 (ASTM., 2010) Type 5 standard. As shown in Figure 2. (a) and (b), respectively. And thus, the second software called Slic3r for slicing and 3D formatting and construction of the parts was used, where the sweep angle adjustment was set to 0º and the model was made with internal filling at 0º alternating with layers with filling at 90º and taken to 3D

printing in the model (Anycubic Mega S, Brazil), with the parameters of table temperature50°C and extruder nozzle 210°C. Figure 2 (c), (d), (e) and (f).

Figure 2 - CP's projection design, (a) specimen in SolidWorck 3D software, (b) Anycubic Mega S 3D printer, ©3D printed specimens, pure PETG CP's, (d) 0.75% NPCu nanocomposite CP's, (e) and 1% NPCu nanocomposite CPs by weight, respectively, (f).

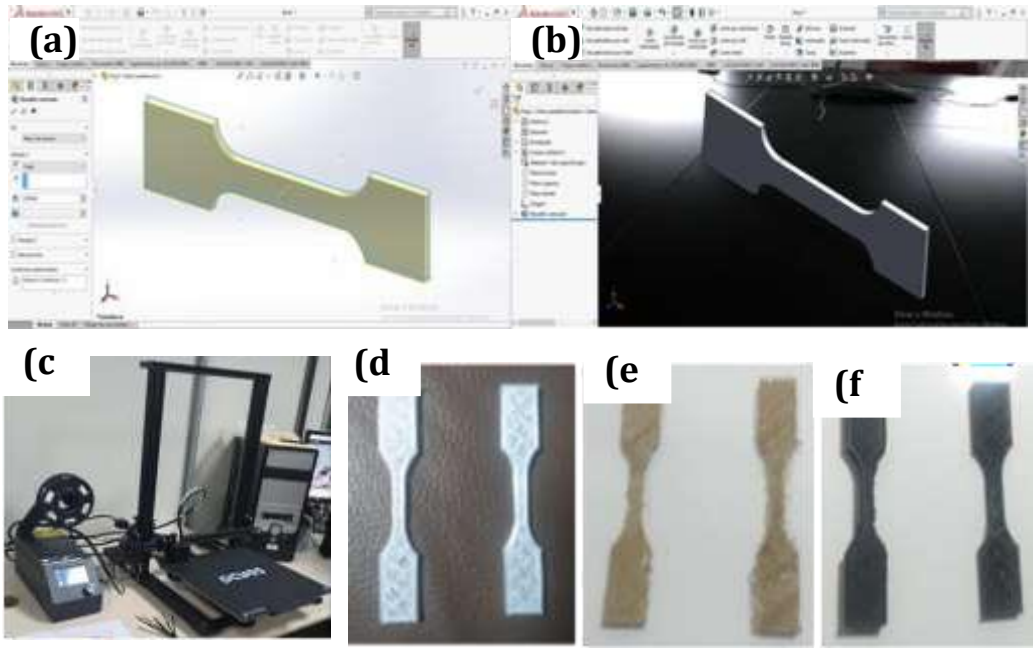

Source: Santos et al (2021).

Mechanical Characterization - Nano hardness

The nanoindentation measurement test was performed with equipment (HM 2000, Fischerscope, Germany) (Vickers hardness test) according to ASTM E 384-17 and ASTM E 2546-15 standards. The load used was 1000 mN, which was applied for 5 seconds to measure the elastic modulus of the materials.

Thermogravimetric analysis - TGA

The equipment (model DTG-60, Shimadzu), provided by the Laboratory of Electrochemistry and Energy - (LEEN) of the Federal University of Amazonas - UFAM, was used to estimate the thermal behavior of the materials with the purpose of obtaining the degradation temperatures of the mass percentage. The test was performed from 25 ºC to 700 ºC, at a heating rate of 20 ºC/min and used a nitrogen atmosphere with a flow rate of 50 mL/min.

Optical Microscopy Analysis

It was used the optical stereomicroscope (MZ 75, Leica) to evaluate the surface in relation to the dispersion of NPCu and the print quality.

Analysis of chemical composition by Fourier Transform Infrared Spectroscopy (FTIR)

An infrared absorption spectroscopy equipment was used (Perkin Elmer, Spectrum One-FTIR Spectrometer, USA). The spectra will be obtained in the form of a KBr pellet in the regionof 4000 to 450 cm 1.

RESULTS AND DISCUSSIONS

The results of the mechanical nanoindentation tests for the pure polymer and the nanocomposites are presented in Table 1. Figures 3 (a-b) show the micrographs of the nanoindentations made on the surfaces of the nanocomposites (0.75 and 1.0% by weight) respectively. From the images it is possible to observe that for figure 3 (a) it presents itself witha shallow depth being noticeable a light tone in the inner folds of the indentation in diamond shape and for figure 3 (b) the indentation is observed with a darker tone presenting a greater depth.

Figure. 3 - Nanoindentation (PETG+NPCu - 0.75% by weight), (a). (PETG + NPCu - 1.00% by weight), (b).

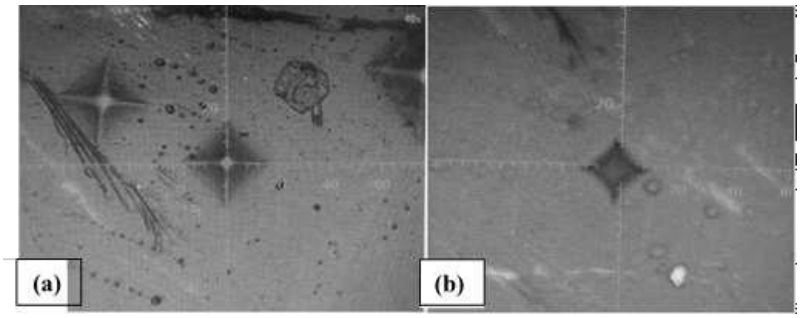

Source: Santos et al (2021).

According to Table 1, it is possible to observe a Young's modulus of 1.48 GPa for the pure polymer (PETG). After the addition of the nanoparticles, the Young's modulus values in the

materials increased. There was an increase of ~9% for the nanocomposite with 0.75% by weight and ~48% for the nanocomposite with 1.0% by weight of NCu. The higher Young's modulus values for the nanocomposites were due to the addition of NanoCu that caused an increase in the degree of crystallinity, indicating that the micronized particles acted as nucleating agents for the crystallization in the material.

Table 1. Mechanical results for pure PETG and NCu nanocomposites

Samples	**Young 's modulus (GPa)**
PETG Pure	1,48
0,75 %	2,60
1%	2,85

Source: Santos et al (2021).

In the characterization by thermogravimetry (TGA), it was possible to examine the thermal stability of pure PETG (without nanoparticle) and composites reinforced with copper nanoparticle (PETG/NPCu). In figure 4, it is observed that the (PETG without nanoparticle) presents two stages of thermal decompositions, where the first stage occurs at an initial temperature of approximately 383ºC with a drop to a secondary temperature with approximately 472ºC and the second stage occurred between the interval of 472ºC and final temperature of approximately 598ºC, with a variation of mass loss of 15%, between 472ºC and 598ºC. Wherefor temperatures higher than 598 ºC shows the total decomposition of the polymer. Similar studies by (V. S. GIITA SILVERAJAH et al, 2012, pp. 5878–5898), state that this event occursdue to the degradation of longer chains of polymeric materials that were not degraded in the first peak.

For the nanocomposites, it can be observed that, after the addition of nanoparticles, the mass loss of PETG occurred with an increase in initial temperatures higher than pure PETG (without nanoparticle), with the initial temperature at 387ºC and final temperature of 478ºC forthe nanocomposite with 0.75% NPCu and initial temperature of 402ºC and final temperature of484ºC for the nanocomposite with 1% NPCu. Thus, this effect may be related to an element ofthe chemical composition of the material, which in this case is exactly the copper nanoparticlethat requires greater thermal energy to fully decompose the initial filament sample or degradation residues according to (PASZKIEWICZ et al, 2017, pp. 41745-41754).

Figure 4 - Thermogravimetric analysis of pure PETG polymer samples, nanocomposite with 0.75% by weight ofNcu, and nanocomposite with 1.0% by weight of NPCu, respectively.

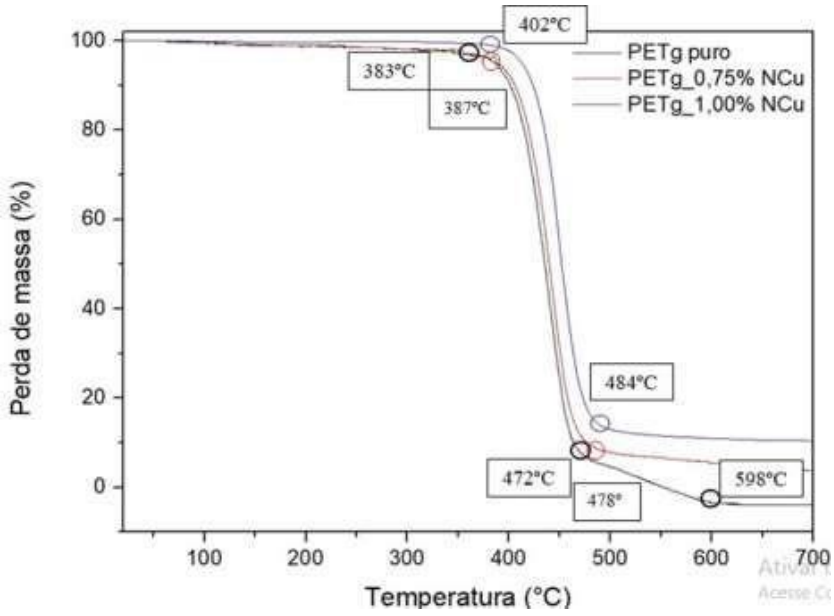

Source: Santos et al (2022).

Fractographic Analysis of Scanning Electron Microscopy - SEM

In the following Figures, the micrographs of the fractures of the 3D printed samples of PETG 0.0% (pure), with addition of 0.75% and 1.00% of copper nanoparticle are presented. Figure 5 (a) (pure PETG) shows the voids or internal voids that occurred due to the choice of slicing of the cross-linked or rotary type with 30% of printing filling defined as standard. These voids did not change in size because they were properly without nanoparticles. Because they resemble the voids called subperimetric, which according to (TAO Y et al, 2019) are formed between rotating rasters along the perimeter of a layer that is commercially known in Additive Manufacturing (AM) technologies as fused filament fabrication (FFF).

Figure 5 (b) (pure PETG 0.0%) shows a smooth and defect-free surface and side and very well compacted filling. Figure 5 (c) shows the effect of the process parameters of the extruder nozzle temperature, which is critical for the print quality, as it determines the printingability by fusion, the raster bond, and the degradation of the raw material. (SPOERK et al, 2017)found that increasing the nozzle temperature improved adhesion and resulted in smaller voids.In addition to decreasing viscosity and increasing flow capacity, higher nozzle temperatures also affect size accuracy and thermal degradation of the polymer.

Figure 5 - Scanning electron microscopy of pure PETG CP (0% Copper Nanoparticle) cross section at 12x, (a)CP in longitudinal section at 16x, (b) CP in lateral section at 20x, respectively (c).

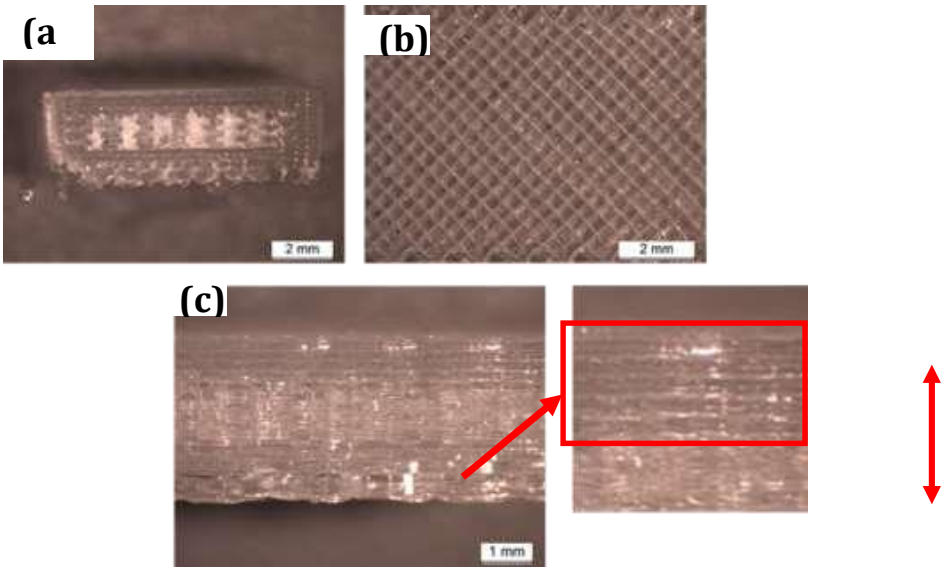

Source: Santos et al (2023).

In Figures 6 (a) and (c), for the samples with 0.75% copper nanoparticle content, it is possible to verify printing defects causing partial voids of growth in the inner central part of the sample. Where (GURRALA PK et al, 2014) state that they can form because of incomplete neck growth between the adjacent interlayer and interlayer rasters (called filaments of the diagram). In Figure 6 (b), it shows the surface with more roughness, with an average length ofthe diameters of the extruded rasters with an increase of 47.45% and with voids due to the rasters that, according to the studies of (RAHIM TNAT et al, 2019) is the perimeter of a layer that is defined by its contour and (VAES D et al, 2021) states that the type of filling as the formof load addition can interfere with the rheology of the material and the thermal and kinetic properties of crystallization.

Figure 6 - Scanning electron microscopy of pure PLA CP + 0.75% Copper Nanoparticle cross section at 12x, (a)CP in longitudinal section at 16x, (b) and lateral section at 20x, respectively (c).

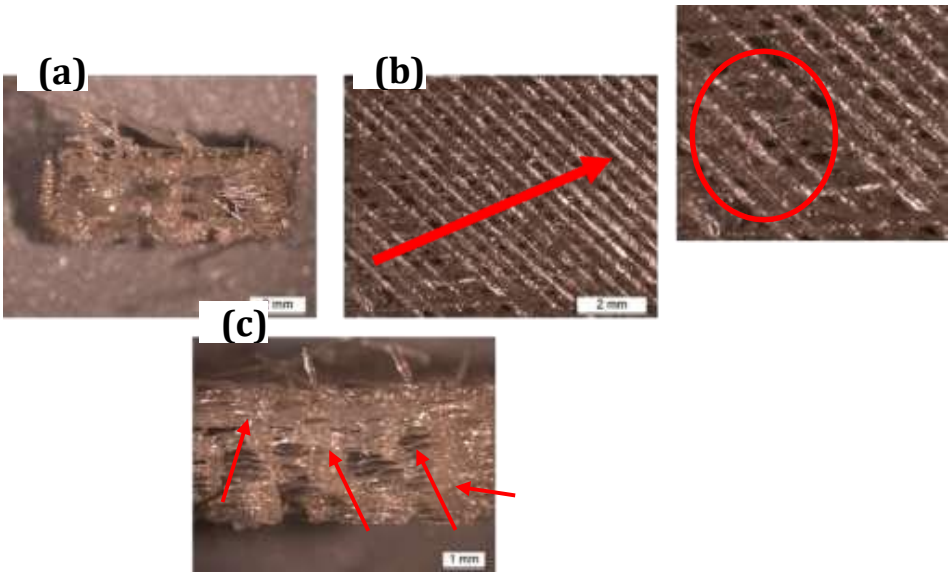

Source: Santos et al (2023).

As can be seen in Figure 7 (a), the intra-sphere voids of the material persist in the multi-scale FFF structure after deposition, according to similar studies by (VAN DE WERKEN N etal, 2020), where the intra-sphere or intra-cord voids are reduced as the temperatures decrease after deposition. However, some voids persist, as the faster cooling rate of the outer raster surface prevents the internal voids from completing the shrinkage. Therefore, the effectivenessof reducing intra-sphere voids in FFF parts of porous materials through the adjustment of the 3D printing process itself is limited according to what (SOMMACAL S et al, 2021) states.

And in Figure 7 (b) it is presented, again, defects and voids rasters on the surface of the piece as shown in the magnification of the figure, because according to studies by (POLYCHRONOPOULOS ND et al, 2020) and (BHALODI D et al, 2019), the rasters would solidify before completing the coalescence and they are also impossible to eliminate entirely due to certain inherent aspects, inevitable characteristics of the FFF process, such as incompletefilling and inconsistent material flow. Already in figure 7 (c), it shows defects of a variation ofadhesion between the layers of the rasters along the height of the piece. Because, according to (HUANG B et al, 2014) it occurs due to the effects of the extruder nozzle temperature, the influence of the table temperature and the printing speed as presented in their works.

Figure 7 - Scanning electron microscopy (SEM) of CP PLA + 1.0% Copper nanoparticle cross-section at 12x, (a) CP in longitudinal at 16x, (b) and lateral at 20x, respectively (c).

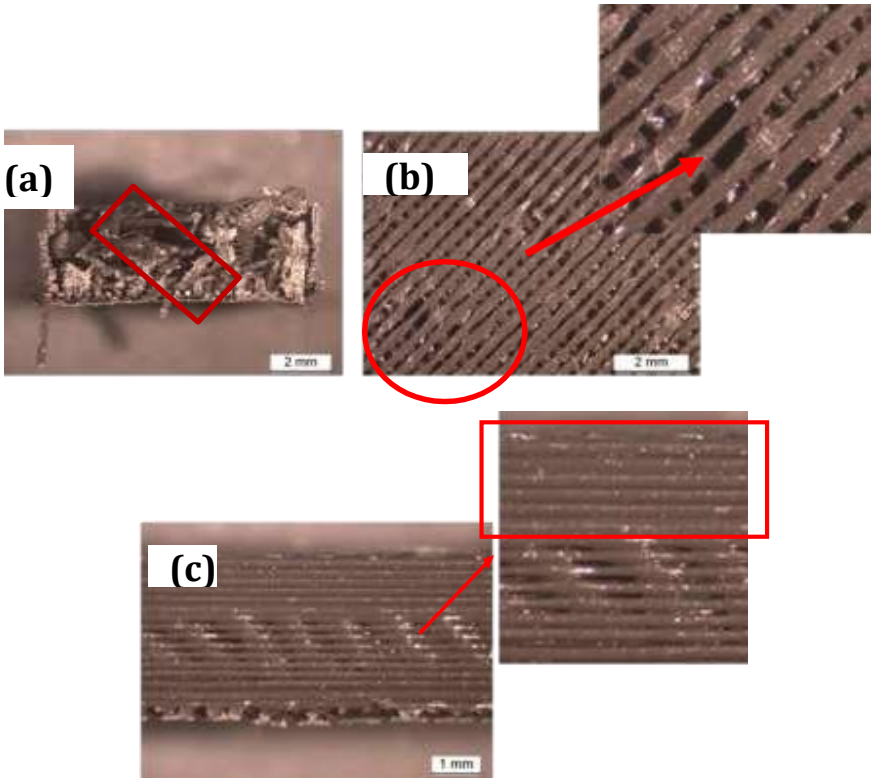

Source: Santos et al (2023).

To contribute to the interpretation of the data obtained in the characterization by Fourier Transform Infrared Spectroscopy (FTIR). According to (A. GUZMÁN D et al, 2015) region1, the characteristic band of (2964 cm^{-1}) is observed and is associated with the stretching of the -CH bond; in region 2, the band in the range of (1712.6) cm^{-1} corresponds to the C=O bond and according to (CHIENG et al, 2014), those in the range between (1408 and 1369) cm^{-1}correspond to the C-H bending. In region 3, the range (1238) cm^{-1} is related to the tension of the =COC bond as stated by (A. GUZMÁN D et al, 2015) and (1098) cm^{-1} corresponds to the -C-O stretching (CHIENG et al, 2014). Finally, the characteristic bands between (968 and 791)cm^{-1} are related to the C-H stretching according to (BITENCOURT et al, 2011).

Figure 8 - FTIR spectra for PETG samples with Copper Nanoparticle and pure Copper Nanoparticle samples.

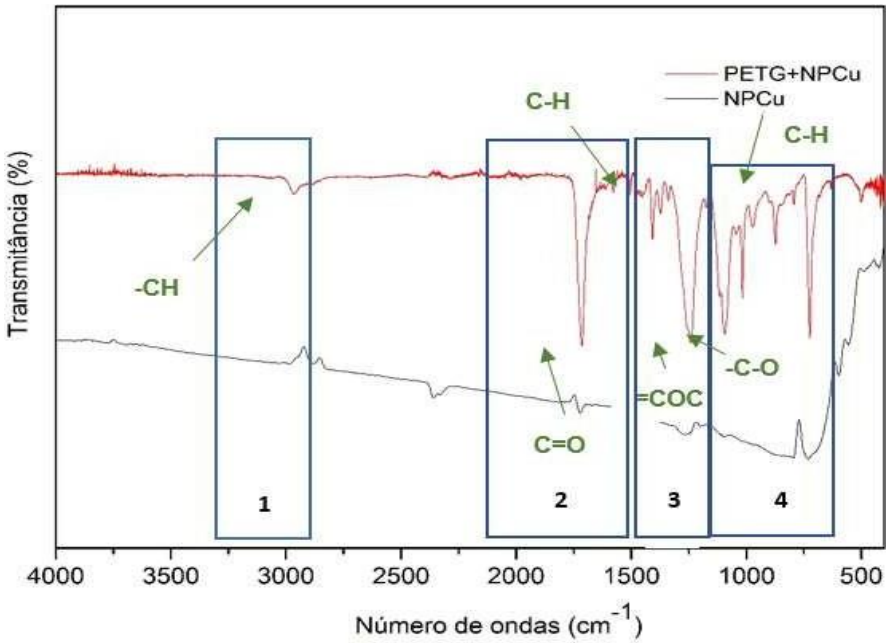

Source: Santos et al (2023).

The FTIR report's wave peak values can be found in the following table 2.

Table 2 - FTIR report's

Wave Number (cm 1)				
Sample	**Region 1**	**Region 2**	**Region 3**	**Region 4**
PETG + NPCu	2964	1712,6; 1408; 1369	1238; 1098; 1014	968; 791; 500

Source: Santos et al (2023).

CONCLUSION

The results obtained in this work are very close to those obtained by other authors who investigated the combined effect. The nano hardness and Young's modulus for pure PETG were 1.48 Gpa and after the addition of Cu nanoparticle, the Young's modulus increased to 2.60 and 2.85 Gpa for 0.75% and 1.0%, respectively. In the Thermogravimetry characterization - (TGA), after the addition of Cu nanoparticle - (NPCu) the mass loss of PETG increased in the second thermal event compared to the nanocomposites with 1% and 0.75% addition of NPCu.

In the factual analysis by scanning electron microscope - (SEM), pure PETG showed internal voids and smaller voids on the side and surface due to the effects of the extruder nozzle temperature parameters of the 3D printer.

In the composite with the addition of 0.75% of copper nanoparticle - (NPCu), the fracture showed defects causing partial voids of growth in the central internal part and on its surface, it showed rougher and with voids due to the raster.

In the composite with the addition of 1% of copper nanoparticle, in the fracture it presents voids called intra-sphere, on its surface it noticed voids of rasters and laterally it presented variation of adhesion between the layers of the raster as the height of the piece duringprinting.

In the chemical composition by FTIR spectrum it was possible to observe that the characteristic bands of the nanocomposite are in accordance with the literature.

The mechanical properties of nano indentation observed for the pure PETG polymer andits nanocomposites, as well as the thermal stability and its chemical composition are similar tothose produced by other techniques. In summary, the products manufactured by 3D printer (PPE) with PETG polymer containing copper nanoparticles can be used by health professionals or in biomedicine.

REFERENCES

Agência Nacional de Vigilância Sanitária – Anvisa. Nota técnica GVIMS/GGTES/ANVISA Nº 05/2020.ANATOL LOCKER.; **ALL3DP**, https://all3dp.com/1/petg-filament-3d-printing/. Acessadoem dezembro de 2017.

ASTM, Standard testsmethod for tensilepropertiesofplastics, United States, **ASTM International**, 2010.

BHALODI, D.; ZALAVADIYA. K: Influence of temperature on polymer parts manufactured by fused deposition modeling process. **J Braz Soc Mech Sci** 2019; 41:113. HTTPS://DOI.ORG/10.1007/S40430-019-1616-Z.

BITENCOURT, S.S.; BATISTA, K.C.; ZATTERA, A.J.; et al., ―Desenvolvimento de biocompósitos de poli (L-ácido láctico) (PLLA) com serragem de madeira‖, **Matéria (R.J.)**, v.22, n.4, Ago. 2017.

CHIENG, B.W.; IBRAHIM, N.A.; THEN, Y.Y.; et al., ―Epoxidized vegetable oils plasticized poly (lactic acid) biocomposites: mechanical, thermal and morphology properties‖, **Molecules**, v.19, n.10, pp. 16024-16038, Oct. 2014.

Compston P. SOMMACAL S.; MATSCHINSKI, A.; DRECHSLER, K.; COMPSTON, P.

Characterisation of void and fiber distribution in 3D printed carbon-fiber/PEEK using X-ray computed tomography. **Compos Part A Appl Sci Manuf** 2021; 149:106487. https:// doi.org/10.1016/j.compositesa.2021.106487.

DE PAOLI, M. A.; Degradação e Estabilizaçãode Polímeros, **Chemkeis,** 2ª ed, 2008. Disponível http://www.chemkeys.com/blog/wpcontent/uploads/2008/09/polimeros.pdf. Acesso em 23 de dezembro de 2017.

E. GUZMAN, J.; CUGNONI, T.; GMUR, P.; BONHOTE, A.; SCHORDERET**.** Sobrevivência desensores de filme PVDF integrados para condições de envelhecimento acelerado em estruturas aeronáuticas/ **aeroespaciais, Smart Mater. Estrutura**. 22 (6) (junho de 2013), https://doi.org/ 10.1088/0964-1726/22/6/065020.

GURRALA, PK.; REGALLA, SP, Part strength evolution with bonding between filaments in fused deposition modelling. **Virtual Phys Prototyp** 2014; 9:141 e9. https://doi.org/10.1080/ 17452759.2014.913400.slic3r.org/

HUANG B, Singamneni S. Raster angle mechanics in fused deposition modelling. **J ComposMater** 2014; 49:363e83. https://doi.org/10.1177/0021998313519153.

JAIMES, JAVIER A.; ANDRÉ.; NICOLE, M.; MILLET, JEAN K.; WHITTAKER, Gary R. Structural modelingof 2019-novel coronavirus (nCoV) spikeproteinreveals a proteolytically-sensitiveactivation loop as adistinguishingfeaturecomparedto SARS-CoVandrelated SARS-like coronaviruses. **Biorxiv**, p. 1-6, 2020.

MARCH 11. **World Health Organization**. Diretor - General'sopeningremar ksatthemediabriefing on COVID -19 -11. 2020

ORGANIZAÇÃO PAN-AMERICANA DA SAÚDE. **COVID-19 (doença causada pelo novo coronavírus).** Brasília, DF, 2020.

PASZKIEWICZ, S., SZYMCZYK, A., PAWLIKOWSKA, D., *et al*., — Synthesis and

characterization of poly (ethylene terephthalate-co-1,4-cyclohexanedimethylene terephtlatate)-*block*-poly (tetramethylene oxide) copolymers‖, **RSC Advances**, v.7, n.66, pp. 41745-41754, Aug. 2017.

POLYCHRONOPOULOS, ND.; VLACHOPOULOS J.; The role of heating and cooling in viscous sintering of pairs of spheres and pairs of cylinders. **Rapid Prototyp J** 2020; 26:719 e 26. https:// doi.org/10.1108/RPJ-06-2019-0162.

RAHIM TNAT.; ABDULLAH, AM.; Md Akil, H.; Recent developments in fused deposition modeling-based 3D printing of polymers and their composites. **Polym Rev** 2019;5 9:589e624.https://doi.org/10.1080/ 15583724.2019.1597883.

SPOERK, M.; ARBEITER, F.; CAJNER, H.; SAPKOTA, J.; HOLZER, C.; Parametric

optimization of intra- and inter-layer strengths in parts produced by extrusion-based additive manufacturing of poly (lactic acid). **J Appl Polym Sci** 2017; 134:45401. https://doi.org/10.1002/app.45401

TAO, Y.; PAM, L.; LIO, D.; LIO, P.; A case study: mechanical modeling optimization ofcellular structure fabricated using wood flour-filled polylactic acid composites with fused deposition modeling. **Compos Struct** 2019; 216:360e5. https://doi.org/ 10.1016/j.compstruct.2019.03.010.

V.S GIITA SILVERAJAD; N. A. IBRAHIM; W. MD ZIN WAN YUNUS; H.A. HASSAN, AND C.B, WOEI; "A comparative study on the mechanical, thermal and morphological characterization of poly (lactic acid)/epoxidized palm oil blend," Int. J. Mol. Sci., vol. 13, no. 5, pp. 5878–5898, 2012.

VAES, D.; VAN, PUYVELDE, P.; Semi-crystalline feedstock for filament-based 3D printing of polymers. **Prog Polym Sci** 2021; 118: 101411. https://doi.org/10.1016/j. progpolymsci.2021.101411.

TEHRANI, M.; Additively manufactured carbon fiber-reinforced composites: state of the art and perspective**. Addit Manuf** 2020; 31: 100962. https://doi.org/ 10.1016/j.addma.2019.100962.